PART 1

Physical Modeling of Energy Piles at Different Scales

Chapter 1

Soil Response under Thermomechanical Conditions Imposed by Energy Geostructures

The foundation of a building represents a connection between the structure and the supporting soil. The mechanical loads coming from the structure are transferred to the soil through it. A number of requirements must be fulfilled to ensure the stability and comfort of the over-structure, the most important of which are (1) the admissible displacements, (2) the acceptable (concrete) stresses and (3) the safety margins with respect to failure [BSI 95]. These aspects are related to the types and properties of the surrounding soils. Data concerning the soil's response must be collected through a geotechnical survey and represent the basis for the design of the required foundations. Therefore, the behavior of the soil plays a primary role in the design of every geostructure, i.e. every structure that transfers a load to the ground. In the case of energy geostructures, an energy supply role is added to the conventional role of the foundation as a structural support. The foundation is thus subjected to both mechanical and thermal loads transmitted from the piles to the ground. This is the main motivation for understanding and modeling the soil's response when subjected to a thermomechanical solicitation. In this chapter, the state of knowledge on the thermomechanical behavior of soils is revised within the framework of energy geostructures. A constitutive model capable of reproducing the described behavior is presented and used to study the response of soils subjected to thermal-stress paths typical of the areas around energy piles.

Chapter written by Alice DI DONNA and Lyesse LALOUI.

1.1. Introduction

Deep foundations are usually used to limit the settlements of buildings, increase capacity with respect to shallow foundations or reach a more resistant layer of soil when the quality of the surface soil is low. Two stages of the geotechnical design of such foundations are related to the behavior of the surrounding soil: the evaluation of the geotechnical bearing capacity and the prediction of displacements. Starting from the equilibrium of a pile (Figure 1.1), the maximum load Q_{LIM} that a pile can support is calculated as:

$$Q_{LIM} = Q_S + Q_P - W_P \quad [1.1]$$

where Q_S is the portion of bearing capacity provided by the friction between the pile and the soil, Q_P is the portion of the bearing capacity provided by the soil below the pile tip and W_P is the pile weight [LAN 99]. A general formula for the calculation of the lateral and base components is:

$$Q_S = \int_0^{\mathrm{H}} \int_0^{2\pi} \sigma'_h \cdot \tan(\delta) \cdot \mathrm{R}\, d\omega dz \quad [1.2]$$

$$Q_P = \int_0^{R} \int_0^{2\pi} (9 \cdot \mathrm{Cu} + \sigma_v) \cdot \mathrm{r}\, d\omega dr \quad [1.3]$$

where H is the pile height, σ'_h is the horizontal effective stress normal to the pile–soil interface, δ is the friction angle at the interface, R is the pile radius, Cu is the undrained shear strength, σ_v is the vertical stress at the pile tip and r, ω and z are the radial, circumferential and vertical cylindrical coordinates, respectively. From these equations, it appears that the lateral resistance depends, apart from the friction angle at the interface, on the stress state at the pile–soil interface, while the tip resistance is directly related to the resistance of the soil below the pile.

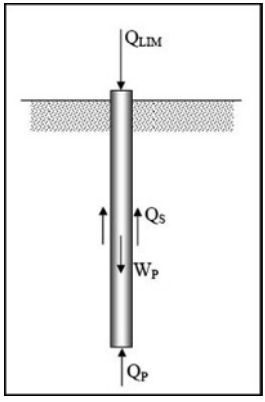

Figure 1.1. *Equilibrium of a pile*

When a thermal load is transmitted from a pile to the soil, the latter reacts by changing its volume, and eventually its response, depending on the type of soil. As a result, the temperature variation can affect (positively or negatively) the stress state at the pile–soil interface and the shear strength that governs tip resistance. More significantly, the thermal volume variation in the soil affects the foundation displacement, making it move upward when the soil dilates and downward when it contracts. The entity of the effects induced by the temperature variations on the behavior of the foundation depends on the volume of heated ground and the range of temperature variation. The thermal load imposed by energy piles in current applications is in the range of 2–30°C (see Chapter 3 for data related to current applications), but future developments using the injection of heat in the ground from other technologies, such as solar panels, will lead to higher temperature variations.

1.2. Thermomechanical behavior of soils

Soils are porous materials made up of a solid skeleton, represented by grains or aggregates, and pores that, in saturated conditions, are filled with water. The case of partial saturation is not considered in this chapter (see Chapter 8 for more details concerning energy piles in unsaturated soils and [FRA 08] for the non-isothermal behavior of unsaturated soils). Soils can be divided into two families: (1) granular (sand and gravel) and (2) fine-grained (silt and clay) materials. Heating a sandy soil in drained conditions results in an increase of volume directly related to the grains' thermal expansion coefficient. Also, water dilates thermal elastically with a thermal expansion coefficient usually higher than that of grains, but due to drained conditions, the water is free to flow away and does not contribute to the volume variation of the material itself. Table 1.1 provides the thermal expansion coefficients of some minerals and water.

Material	Volumetric thermal expansion coefficient [$10^{-6}°C^{-1}$]
Muscovite	24.8
Kaolinite	29.0
Chlorite	31.2
Illite	25.0
Smectite	39.0
Water	139 + 6.1·T

Table 1.1. *Volumetric thermal expansion coefficients (T stands for temperature) [MCK 65, DIX 93]*

The response of clays is more complicated and will be discussed in the next section. The complexity of clayey materials' thermomechanical behavior is a direct

consequence of their microstructure and the electrochemical equilibrium between clay particles. Details about this aspect can be found, among others, in [HUE 92].

1.2.1. *Thermomechanical behavior of clays*

As for granular materials, the two constituents of saturated fine-grained materials (grains/aggregates and water) undergo thermoelastic expansion when heated. However, it has been proved through experimental testing that either a contractive or a dilative volume variation can be observed during heating in drained conditions depending on the load history. The latter is commonly described through the overconsolidation ratio (OCR), defined as:

$$\mathrm{OCR} = \frac{\sigma'_p}{\sigma'_v} \qquad [1.4]$$

where σ'_p is the preconsolidation stress and σ'_v is the current vertical effective stress. The preconsolidation stress is the maximum vertical stress that the soil has already supported (load history). The soil retains a memory of the maximum charge that it has already supported, so that if it is subjected to a load lower than the preconsolidation stress, its deformation is relatively small and, above all, reversible (elastic). If the applied load reaches and surpasses the initial preconsolidation stress, the deformation becomes more significant and, above all, partially irreversible (elastoplastic). In this sense, the preconsolidation stress corresponds to the maximum experienced density (or the lowest void ratio). From a mechanical point of view, it is used to be defined as the limit between the elastic and elastoplastic domains in terms of applied stresses. A soil is considered normally consolidated (NC) if the OCR is within the range of 1 and 2; i.e., if the current load is close to the maximum that the soil has ever supported. Conversely, the material is said to be overconsolidated (OC) if the OCR is greater than 2; i.e., if the current load is lower than the historical maximum. In terms of a fine-grained soil's response to a temperature variation in drained conditions, it has been largely demonstrated that the material contracts upon heating in NC conditions and a significant part of this deformation is irreversible, while highly OC materials experience a volume expansion during heating that is recovered during cooling. Between these two extreme cases, there is an intermediate case represented by slightly OC clays. In this case, the material shows initial dilation and subsequent contraction during heating, followed by contraction during cooling, thus representing a transition between the two main cases. The first experimental results of this nature date back to between the 1960s and 1980s [CAM 68, PLU 69, DEM 82, DES 88, BAL 88] and have been widely confirmed more recently [MIL 92, TOW 93, BUR 00, CEK 04]. Similar results have been obtained by the authors for a wide range of different clayey materials containing variable quantities of illite, kaolinite, chlorite and smectite. Some examples are given in Figure 1.2. In other words, these experimental results

show that a soil can undergo irreversible deformation due to an increase in temperature under a constant mechanical load equal to (see NC cases in Figure 1.2) or even slightly lower than the preconsolidation stress (see cases with OCR = 2 in Figure 1.2). A number of experimental studies on various clays have been performed to develop a theoretical framework for describing this phenomenon, and have led to the conclusion that the "apparent" preconsolidation stress decreases at constant void ratio with increasing temperature. The word "apparent" is used to underline the fact that the applied mechanical load does not change, so that the maximum load historically applied is always the same. Some of these results are summarized and compared in Figure 1.3.

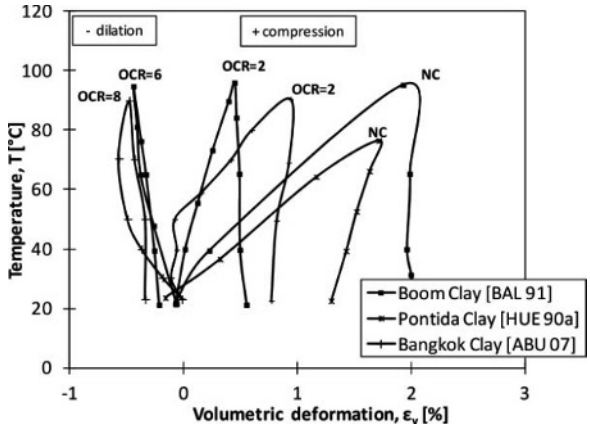

Figure 1.2. *Thermal deformation of various clays under different initial conditions*

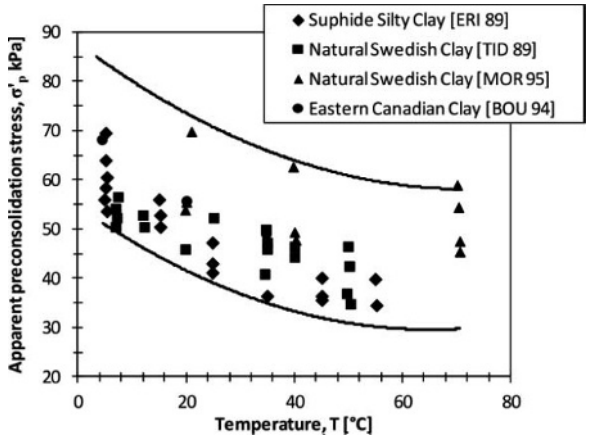

Figure 1.3. *Influence of temperature on preconsolidation pressure [LAL 03]*

To fit these results within a theoretical-schematized framework, the evolution of the apparent preconsolidation pressure can be plotted in the mean effective stress-temperature plane, as shown in Figure 1.4, where the mean effective stress p' is defined as:

$$p' = \frac{\sigma'_v + 2 \cdot \sigma'_h}{3} \quad [1.5]$$

The isotropic preconsolidation pressure, or the maximum mean effective stress that the soil has ever supported, is considered in this plane. As discussed earlier, and in light of the results illustrated so far, the (apparent) preconsolidation pressure represents the limit between the elastic and elastoplastic domains. In Figure 1.4, point A represents the state of a material subjected to an initial temperature (T_0) and an OC stress state, as its current mechanical load (p'_A) is lower than the preconsolidation pressure (p'_{prec}). If this material is subjected to drained heating under a constant mean effective stress p'_A, it will move from A to A'. This thermal-stress path remains inside the elastic domain and the material therefore reacts elastically (cases with OCR = 6 or 8 in Figure 1.2). However, considering an NC (point B) or slightly OC (point C) material, heating induces thermoplastic strain as the thermal-stress paths (i.e. B-B' or C-C') encounter the border of the elastic domain. In the NC case, the material responds elastoplastically from the first temperature increment because its initial stress state is already on the border between the two domains (NC cases in Figure 1.2). In the slightly OC case, the response of the material is initially elastic (up to C'' in Figure 1.4) and then elastoplastic (cases with OCR = 2 in Figure 1.2). The reduction in the apparent preconsolidation pressure, or that of the elastic domain, with temperature is known as thermal softening.

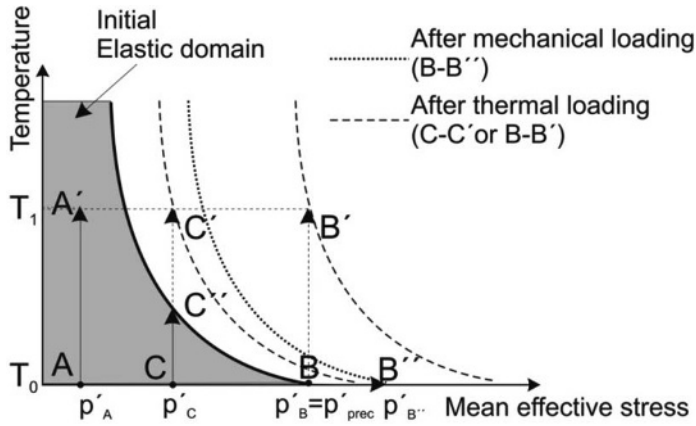

Figure 1.4. *Thermal-stress paths in the mean effective stress-temperature plane*

This phenomenon is opposite of the so-called strain hardening, or the increase of the elastic domain due to the development of irreversible deformations. This latter phenomenon can be explained by simply going back to the definition of preconsolidation stress. If an NC material (point B in Figure 1.4) is mechanically loaded (stress path B-B"), the current applied stress becomes the new preconsolidation stress (the maximum historically applied stress). The increase of the preconsolidation pressure from p'_B to $p'_{B''}$ corresponds to an increase in the elastic domain. The same phenomenon occurs for thermal loading, so that the thermal paths that induce plasticity (C"-C' and B-B' in Figure 1.4) also induce an increase in the elastic domain (from the continuous line to the dotted lines in Figure 1.4).

When non-isotropic stress states are considered, the elastic domain can be represented in a tridimensional space by adding an axis to the plane representation illustrated in Figure 1.4. This third axis corresponds to the deviatoric stress (invariant) q, defined as:

$$q = \sqrt{\frac{3}{2}}\sqrt{\mathrm{tr}(d\mathbf{s})^2} \qquad [1.6]$$

where tr represents the trace of the tensor and **s** the deviatoric stress tensor. The thermal softening is also represented in this space by the shrinkage of the elastic domain with increasing temperature (Figure 1.5). The main consequence of thermal softening under deviatoric stress states is that if an OC material (with a certain void ratio) is sheared at a high temperature (stress path A′-A″), it reaches the border between the elastic and the elastoplastic domains at a lower deviatoric stress with respect to shearing at the initial temperature (stress path A-A‴).

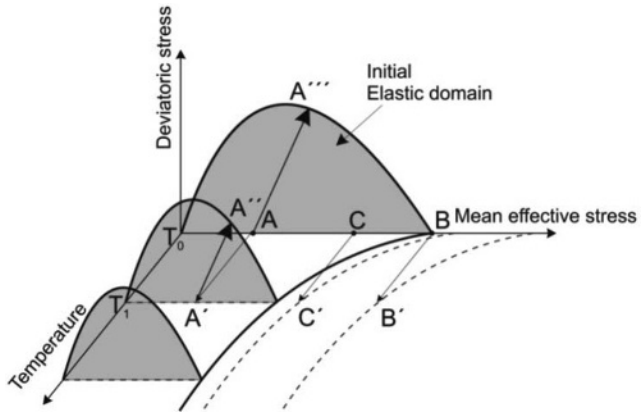

Figure 1.5. *Thermal-stress paths in the mean effective stress–deviatoric stress-temperature space*

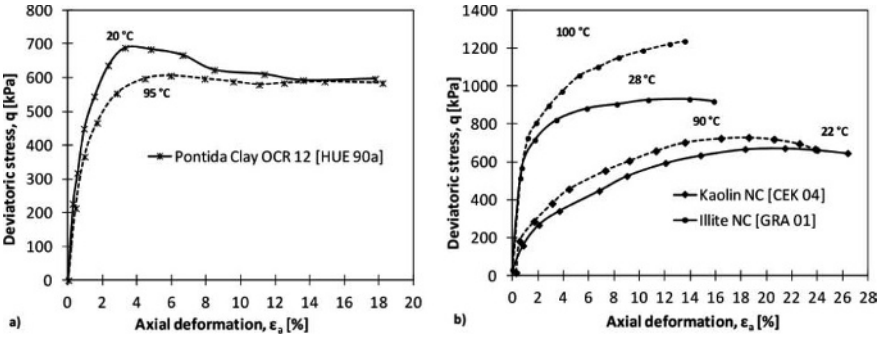

Figure 1.6. *Shear strength at different constant temperatures of a) OC and b) NC clays*

In other words, the material undergoes plasticity earlier than in the isothermal case. Conversely, in the case of an NC or slightly OC material, heating results in a combination of thermal softening and strain hardening. An in-depth analysis of this phenomenon can be found in [HUE 09], and Figure 1.6 illustrates some of those aspects. Within the framework of energy geostructures, the behavior of soils during seasonally cyclic thermal loading is as important as that of the response during a single monotonic heating. Campanella and Mitchell [CAM 68] and Hueckel and Baldi [HUE 98] have shown that the first temperature cycle removes most of the irreversible volume change in NC clays and that subsequent cycles of the same magnitude and range produce small increments of irreversible deformation that decrease cycle after cycle, revealing an accommodation phenomenon. This result is shown in Figure 1.7(a) for illite [CAM 68] and Figure 1.7(b) for a carbonate clay [HEU 98]. Thus, when remaining in the same theoretical framework (Figures 1.4 and 1.5), it is expected that the initial OCR also has an effect on the shear strength of the material at ambient temperature after the application of one or more thermal cycles. If the material is initially OC, a heating-cooling cycle (stress path A-A'-A in Figure 1.4) does not produce any plastic deformation, so that the dimension of the elastic domain after the entire cycle, and thus the response under shearing, is not affected because no permanent change is induced on the void ratio. Conversely, if an initially NC or slightly OC material is subjected to a heating-cooling cycle (B-B′-B or C-C′-C in Figure 1.4), strain hardening occurs as plastic deformation is produced. The material ends up being OC (at an ambient temperature T_0), and this process is generally called thermally induced overconsolidation. To illustrate this phenomenon experimentally, Abuel-Naga *et al*. [ABU 06] has performed a series of tests on an NC soft clay. The result is shown in Figure 1.8(a), which illustrates the effect of one thermal cycle on the oedometric consolidation curve of Bangkok clay. In this test, a conventional oedometric consolidation was run up to 100 kPa at an initial temperature of 22°C (from point 1 to 2). Next, the sample was heated to 90°C and cooled back to the initial temperature (from point 2 to 3). Finally, the consolidation

was continued up to 200 kPa (from point 3 to 5). The results plotted in the figure confirm that the thermal cycle induced a thermal overconsolidation: when mechanical consolidation restarted after the thermal cycle (point 3), a higher stress was needed to plastify again (from 3 to 4). Coherently with the results presented in Figure 1.2, the volume decreased during the thermal cycle (from 2 to 3). As expected, the thermally induced consolidation also resulted in an increase in shear strength. An experimental example of this behavior has been provided by Burghignoli *et al*. [BUR 00], who have showed that if an NC sample is heated and then cooled in drained conditions and tested in a triaxial apparatus, its undrained shear strength is higher than that of an equivalent sample tested at constant ambient temperature (Figure 1.8(b)). At the same time, for instance, an increase in shear strength due to thermal consolidation would improve tip resistance.

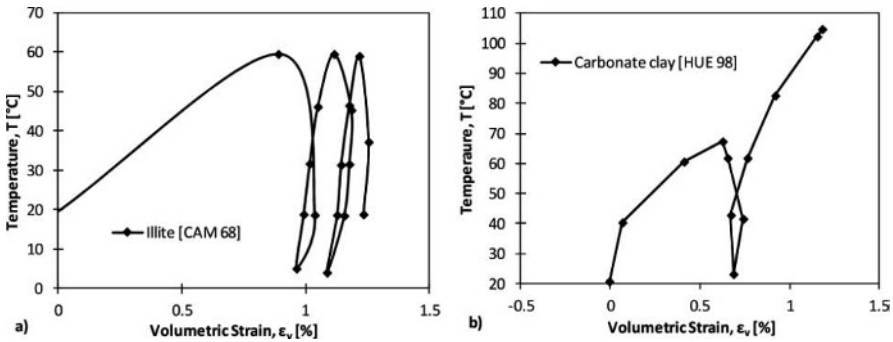

Figure 1.7. *Thermal cyclic effects on NC clays*

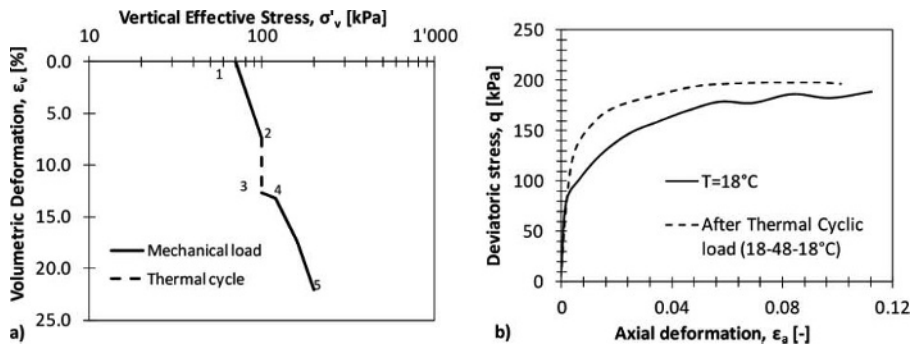

Figure 1.8. *Thermal cyclic effects on a) consolidation of NC Bangkok clay [ABU 06] and b) undrained shear resistance of NC Tody clay [BUR 00]*

1.3. Constitutive modeling of the thermomechanical behavior of soils

This section provides a soil constitutive model with the above-mentioned features and some numerical results. Several constitutive models for describing the thermomechanical behavior of soils have been proposed in the last two decades. A comprehensive summary of their features, capabilities and limitations is presented by Hong *et al*. [HON 13]. Among these models, the model proposed by Laloui *et al*. [LAL 09] is described here.

1.3.1. *The ACMEG-T model*

The Advanced Constitutive Model For Environmental Geomechanics – Thermal effects (ACMEG-T) belongs to the Cam-clay family and is based on the critical state theory. The isothermal part is based on the works of Hujeux [HUJ 79]. Various successive improvements [LAL 93, MOD 97, LAL 08, LAL 09, DI 13] have been made to extend the model's use to non-isothermal conditions. According to the elastoplasticity theory, the tensor of the total strain increment $\mathbf{d\varepsilon}$ is divided into elastic $\mathbf{d\varepsilon^e}$ and plastic $\mathbf{d\varepsilon^p}$ components, so that:

$$\mathbf{d\varepsilon} = \mathbf{d\varepsilon^e} + \mathbf{d\varepsilon^p} \qquad [1.7]$$

The increment of total deformation is composed of volumetric $d\varepsilon_v$ and deviatoric $d\varepsilon_d$ parts, so that:

$$\mathbf{d\varepsilon} = \frac{d\varepsilon_v}{3}\mathbf{I} + \mathbf{de} \quad \text{with} \quad d\varepsilon_v = \mathrm{tr}(\mathbf{d\varepsilon}) \quad \text{and} \quad d\varepsilon_d = \frac{\sqrt{6}}{3}\sqrt{\mathrm{tr}(\mathbf{de})^2} \qquad [1.8]$$

where $\mathbf{I}$ represents the unitary tensor and $\mathbf{de}$ represents the deviatoric strain increment tensor. The Terzaghi formulation for the effective stresses is introduced, so that:

$$\boldsymbol{\sigma}' = \boldsymbol{\sigma} - p_w\mathbf{I} \qquad [1.9]$$

where $\boldsymbol{\sigma}'$and $\boldsymbol{\sigma}$ are the effective and total stress tensors, respectively, and p_w is the pore water pressure. As already mentioned (equations [1.5] and [1.6]), the effective stress increment tensor can be split into the mean effective stress increment dp' and the deviatoric stress increment dq (invariant):

$$\mathbf{d\sigma}' = dp'\mathbf{I} + \mathbf{ds} \qquad [1.10]$$

where $\mathbf{ds}$ is the deviatoric stress increment tensor. In the elastic non-isothermal domain, the increments of volumetric and deviatoric deformation are equal to:

$$d\varepsilon_v^e = \frac{dp'}{K_s} - \beta'_s dT \quad \text{and} \quad d\varepsilon_d^e = \frac{dq}{3G_s} \qquad [1.11]$$

where K_s is the bulk modulus, β'_s is the volumetric thermal expansion coefficient, T is the temperature and G_s is the shear modulus. The nonlinear elastic response is obtained through the following equations:

$$K_s = K_{ref}\left(\frac{p'}{p'_{ref}}\right)^{n_e} \text{ and } G_s = G_{ref}\left(\frac{p'}{p'_{ref}}\right)^{n_e} \quad [1.12]$$

where K_{ref} and G_{ref} are the two moduli at the reference mean effective stress p'_{ref} and n_e is a material parameter. The plastic response is described by two mechanisms, one isotropic and one deviatoric, that are coupled. Purely isotropic loading causes only volumetric plastic deformation, while purely deviatoric loading causes both deviatoric and volumetric plastic deformation. The two yield surfaces are represented in the p′-q-T space at constant void ratio in Figure 1.9(a). Both are temperature dependent, so that when a thermomechanical load leads the stress point on one of these two surfaces, thermal plastic deformation (contraction) is developed. The isotropic yield limit is:

$$f_{iso} = p' - p'_c r_{iso} = 0 \quad [1.13]$$

where r_{iso} is the isotropic mechanism's degree of mobilization of plasticity (bounding surface theory [DAF 80]). The yield limit evolves with the volumetric plastic deformation induced by the isotropic mechanism $\varepsilon_v^{p,iso}$, as:

$$r_{iso} = r_{iso}^e + \frac{\varepsilon_v^{p,iso}}{c+\varepsilon_v^{p,iso}} \quad [1.14]$$

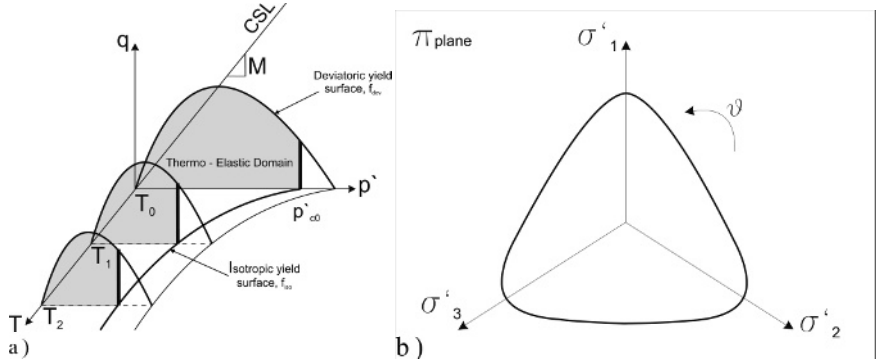

Figure 1.9. *ACMEG-T model (T2>T1>T0): a) representation of the isotropic and deviatoric yield limits as functions of temperature and b) van Eekelen surface and plane strain stress path in the deviatoric plane*

where r_{iso}^e is the initial value of the degree of mobilization of plasticity and c is a material parameter. In this model, the dependence of the preconsolidation pressure

on temperature (thermal softening) and its evolution with the development of the volumetric plastic deformation (strain hardening) is expressed as [LAL 03]:

$$p'_c = p'_{c0} e^{\beta \varepsilon_v^p} \left[1 - \gamma_T \cdot \ln\left(\frac{T}{T_0}\right)\right] \quad [1.15]$$

where p'_{c0} and T_0 are the initial preconsolidation pressure and temperature, respectively, β is the plastic index, ε_v^p is the total volumetric plastic deformation and γ_T is a material parameter that defines the shape of the isotropic yield function with respect to temperature (horizontal plane in Figure 1.9(a) or Figure 1.4). The deviatoric yield limit is:

$$f_{dev} = q - Mp' \left(1 - b \cdot \ln\left(\frac{d \cdot p'}{p'_c}\right)\right) r_{dev} = 0 \quad [1.16]$$

where M is the slope of the critical state line (CSL) in the p'-q plane (Figure 1.9(a)), b and d are two material parameters and r_{dev} is the deviatoric mechanism's degree of mobilization of plasticity. The latter has the same role as r_{iso} and is given by:

$$r_{dev} = r_{dev}^e + \frac{\varepsilon_d^p}{a + \varepsilon_d^p} \quad [1.17]$$

where a is a material parameter, r_{dev}^e is the initial value of the degree of mobilization of plasticity and ε_d^p is the deviatoric plastic deformation. The parameter d represents the ratio between the preconsolidation and the critical pressure p'_{cr}, as:

$$d = \frac{p'_c}{p'_{cr}} \quad [1.18]$$

The coefficient M depends on the Lode angle ϑ to account for the effect of the stress path direction in the π plane (Figure 1.9(b)), perpendicular to the space diagonal [POT 99]. This model adopts the formulation proposed by van Eekelen [VAN 80], in which the M coefficient is defined as:

$$M = 3\sqrt{3} \cdot a_L \left(1 + b_L \cdot \sin(3\vartheta)\right)^{n_L} \quad [1.19]$$

where a_L, b_L and n_L are three material parameters. The first and second of these parameters depend on the friction angles in compression and extension, φ_c and φ_e, respectively, so that by defining:

$$r_c = \frac{1}{\sqrt{3}}\left(\frac{2 \cdot \sin\varphi_c}{3 - \sin\varphi_c}\right) \text{ and } r_e = \frac{1}{\sqrt{3}}\left(\frac{2 \cdot \sin\varphi_e}{3 + \sin\varphi_e}\right) \quad [1.20]$$

they become:

$$b_L = \frac{\left(\frac{r_c}{r_e}\right)^{1/n_L} - 1}{\left(\frac{r_c}{r_e}\right)^{1/n_L} + 1} \quad \text{and} \quad a_L = \frac{r_c}{(1+b_L)^{n_L}}$$
$$\text{with } a_L > 0;\ \ b_L n_L > 0;\ -1 < b_L < 1 \qquad [1.21]$$

The value of n_L must be assumed to ensure the convexity condition [BAR 98], and the Lode angle is defined as:

$$\sin(3\vartheta) = -\left(\frac{3\sqrt{3}}{2}\frac{III_s}{II_s^3}\right) \text{ with } II_s = \frac{1}{2}\boldsymbol{s_{ij}s_{ij}} \text{ and } III_s = \frac{1}{3}\boldsymbol{s_{ij}s_{jk}s_{ki}} \qquad [1.22]$$

where IIs and IIIs are the second and third invariants of the deviatoric stress tensor, respectively. The flow rule is associated for the isotropic mechanism, but unassociated for the deviatoric mechanism, which means that when referring to the isotropic and deviatoric plastic potentials as g_{iso} and g_{dev} respectively, $g_{iso} = f_{iso}$ but $g_{dev} \neq f_{dev}$, as [NOV 79]:

$$g_{dev} = q - \frac{\alpha}{\alpha-1} M p' \left[1 - \frac{1}{\alpha}\left(\frac{d\cdot p'}{p'_c}\right)^{\alpha-1}\right] = 0 \qquad [1.23]$$

where α is a material parameter that expresses the dilatancy rule:

$$\frac{d\varepsilon_v^p}{d\varepsilon_d^p} = \alpha\left(M - \frac{q}{p'}\right) \qquad [1.24]$$

The flow rules for the volumetric and deviatoric plastic strains are:

$$d\varepsilon_v^p = \lambda_{iso}^p \frac{\partial g_{iso}}{\partial p'} + \lambda_{dev}^p \frac{\partial g_{dev}}{\partial p'} \qquad [1.25]$$

$$d\varepsilon_d^p = \lambda_{dev}^p \frac{\partial g_{dev}}{\partial q} \qquad [1.26]$$

where λ_{iso}^p and λ_{dev}^p are the plastic multipliers for the isotropic and deviatoric mechanisms, respectively. These multipliers can then be calculated by starting from the consistency equation:

$$d\mathbf{f} = \frac{\partial \mathbf{f}}{\partial \boldsymbol{\sigma}'} : d\boldsymbol{\sigma}' + \frac{\partial \mathbf{f}}{\partial T} dT + \frac{\partial \mathbf{f}}{\partial \boldsymbol{\varepsilon}^p} : d\boldsymbol{\varepsilon}^p \qquad [1.27]$$

where **f** is the vector that includes the two yield surfaces f_{iso} and f_{dev}. The second term on the right side of equation [1.27] is responsible for the thermoplastic component of the deformation. To account for cyclic effects, the degree of plastification for the isotropic yield mechanism changes during thermal cycles. No

further thermoplastic deformation is added after a certain number of cycles, unless the maximum temperature imposed during the previous cycle is exceeded. This model reproduces the cyclic thermal accommodation phenomenon experienced by soils (Figure 1.7).

1.3.1.1. *Numerical analyses with the ACMEG-T model*

The model has been validated by Laloui *et al*. [LAL 09] and shown to be capable of reproducing the experimental results under different thermal-stress paths with good accuracy. The purpose here is to illustrate the model's performance under thermal and mechanical loading conditions similar to those imposed by energy piles. In this sense, the analysis focuses on (1) the volume variation under heating and cooling cycles and (2) the shear strength at different temperatures. The first aspect is more related to the thermally induced displacement of the foundation and the thermal effect on the stress state at the pile–soil interface, while the second aspect is more related to the pile tip response. Therefore, three examples of simulations run with the ACMEG-T model are studied to reproduce three experimental results on Boom [BAL 91] and Bangkok [ABU 06] clays. The ACMEG-T parameters of the two considered materials are listed in Table 1.2. These parameters were previously calibrated based on the experimental data available in the literature. The procedure for calibration can be found in [LAL 09]. The first case includes three tests (one NC and two OC) run on Boom clay by imposing one drained heating–cooling cycle from 20 to 95°C under constant isotropic confinement. The confinement imposed for the NC conditions was 6 MPa, while in the two OC cases, the sample was first consolidated to 6 MPa and then unloaded to 3 (OCR = 2) and 1 MPa (OCR = 6). Identical thermal-stress paths were numerically simulated with ACMEG-T, and the results, presented in Figure 1.10(a), show the ability of the model to develop thermoelastic or thermoelastoplastic deformation depending on the material's initial OCR. The second case, related to the thermal volume change of clays, concerns the test performed on Bangkok clay and already shown in Figure 1.8(a). The entire process is simulated, starting from an initial consolidation from 70 to 100 kPa, then the application of one thermal cycle (22–90–22°C) in drained conditions and the continuation of consolidation up to 200 kPa. The numerical results are shown in Figure 1.10(b) and match the experimental data, illustrating the model's ability to reproduce the thermal consolidation phenomenon discussed in this chapter.

Finally, the experimental results provided by Abuel-Naga *et al*. [ABU 06] on NC Bangkok clay were considered to check the model's ability to reproduce the responses under triaxial conditions at different temperatures. The tests are run for consolidation under an isotropic mean effective stress of 300 kPa and then sheared under an axial strain control of up to 30%. The comparison between the experimental and numerical results is shown in Figure 1.11(a) in terms of deviatoric stress and in Figure 1.11(b) in terms of volumetric deformation.

Isothermal elastic parameters			**Boom**	**Bangkok**
Bulk modulus at $p'_{ref} = 1$ MPa	K_{ref}	[MPa]	130	42
Shear modulus at $p'_{ref} = 1$ MPa	G_{ref}	[MPa]	130	15
Elastic exponent	n_e	[-]	0.4	1
Thermal elastic parameters				
Thermal expansion coefficient	β'_s	[°C^{-1}]	4×10^{-5}	2×10^{-4}
Isothermal plastic parameters				
Material parameters	a	[-]	0.007	0.02
	b	[-]	0.6	0.2
	c	[-]	0.012	0.04
	d	[-]	1.3	1.6
Friction angle in compression	φ'_c	[°]	16	22.66
Friction angle in tension	φ'_e	[°]	16	22.66
Lode parameter	n_L	[-]	–0.229	–0.229
Dilatancy parameter	α	[-]	1	2
Plastic index	β	[-]	18	5.49
Initial isotropic plastic radius	r^e_{iso}	[-]	0.001	0.15
Initial deviatoric plastic radius	r^e_{dev}	[-]	0.3	0.1
Thermal plastic parameters				
Evolution of f_{iso} with temperature	γ_T	[-]	0.2	0.22

Table 1.2. *ACMEG-T parameters for Boom and Bangkok clays*

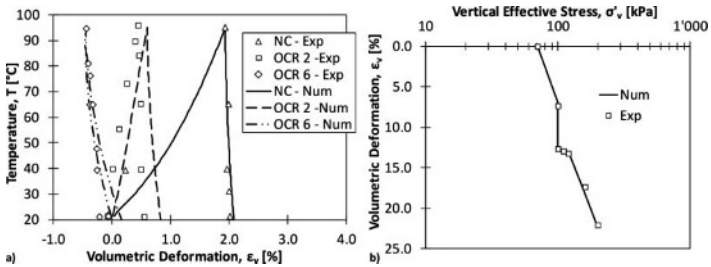

Figure 1.10. *Numerical simulations with ACMEG-T: (a) thermal deformation of Boom clay [BAL 91] and (b) thermal consolidation of Bangkok clay [ABU 06]*

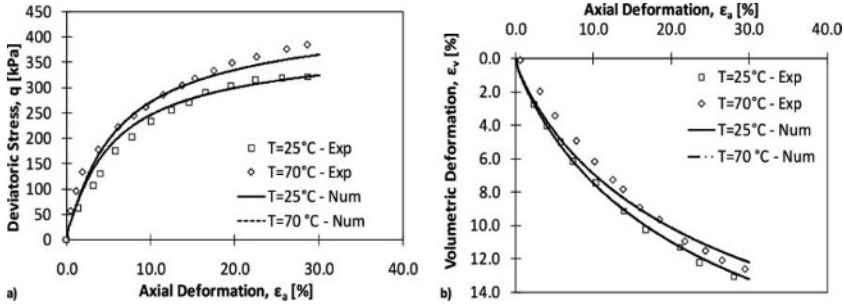

Figure 1.11. *Numerical simulations with ACMEG-T: drained triaxial tests on Bangkok clay at different temperatures [ABU 06]*

1.4. Acknowledgments

This research project was funded by the Swiss Federal Office of Energy (contract no. 154,426).

1.5. Bibliography

[ABU 06] ABUEL-NAGA H.M., BERGADO D.T., RAMANA G.V., *et al.*, "Experimental evaluation of engineering behaviour of soft Bangkok clay under elevated temperature", *Journal of Geotechnical and Geoenvironmental Engineering*, vol. 132, no. 7, 2006.

[ABU 07] ABUEL-NAGA D.T., BERGADO A., BOUAZZ A., "Thermally induced volume change and excess pore water pressure of soft Bangkok clay", *Engineering Geology*, vol. 89, pp. 144–154, 2007.

[BAL 88] BALDI G., HUECKEL T., PELLEGRINI R., "Thermal volume changes of mineral water system in low porosity clay soils", *Canadian Geotechnical Journal*, vol. 25, pp. 807–825, 1998.

[BAL 91] BALDI G., HUECKEL T., PEANO A., *et al.*, *Developments in Modelling of Thermo-Hydro-Mechanical Behaviour of Boom Clay and Clay-Based Buffer Materials (vols. 1 and 2)*, EUR 13365/1 and 13365/2, Luxembourg, 1991.

[BAR 98] BARNICHON J.D., Finite element modelling in structural and petroleum geology, Doctoral Thesis, Faculty of Applied Sciences, University of Liege, 1998.

[BOU 94] BOUDALI M., LEROUEIL S., SRINIVAS A., *et al.*, "Viscous behaviour of natural clays", *Proceedings of the 13th International Conference on Soil Mechanics and Foundation Engineering*, vol. 1, New Delhi, India, pp. 411–416, 1994.

[BUR 00] BURGHIGNOLI A., DESIDERI A., MILIZAINO S., "A laboratory study on the thermo mechanical behaviour of clayey soils", *Canadian Geotechnical Journal*, vol. 37, pp. 764–780, 2000.

[BSI 95] BSI (British Standards Institution), *Eurocode 7: Geotechnical Design*, London, 1995.

[CAM 68] CAMPANELLA R.G., MITCHELL J.K., "Influence of the temperature variations on soil behaviour", *Journal of the Soil Mechanics and Foundation Engineering Division*, vol. 94, no. SM3, pp. 709–734, 1968.

[CEK 04] CEKEREVAC C., LALOUI L., "Experimental study of thermal effects on the mechanical behaviour of a clay", *International Journal of Numerical and Analytical Method in Geomechanics*, vol. 28, no. 3, pp. 209–228, 2004.

[DAF 80] DAFALIAS Y., HERRMANN L., "A bounding surface soil plasticity model", *International Symposium on Soils Under Cyclic and Transient Loading*, Swansea, pp. 335–345, 1980.

[DEM 82] DEMARS K.R., CHARLES R.D., "Soil volume changes induced by temperature cycling", *Canadian Geotechnical Testing Journal*, vol. 19, pp. 188–194, 1982.

[DES 88] DESIDERI A.,"Determinazione sperimentale dei coefficienti di dilatazione termica delle argille", *Proceedings Convengo del Gruppo Nazionale di Coordinamento per gli Studi di Ingegneria Geotecnica*, vol. 1, *sul tema: Deformazioni dei terreni ed interazione terreno-struttura in condizioni di esercizio*, Monselice, Italy, pp. 193–206, 5–6 October 1988.

[DI 13] DI DONNA A., DUPRAY F., LALOUI L. "Numerical study of the effects induced by thermal cyclic soil plasticity on the geotechnical design of energy piles", *Computers and Geotechnics*, 2013, in press.

[DIX 93] DIXON D., GRAY M., LINGNANU B., *et al.*, "Thermal expansion testing to determine the influence of pore water structure on water flow through dense clays", *46th Canadian Geotechnical Conference*, Saskatoon, pp. 177–184, 1993.

[ERI 89] ERIKSSON L.G., "Temperature effects on consolidation properties of sulphide clays", *12th International Conference on Soil Mechanics and Foundation Engineering*, vol. 3, Rio de Janeiro, pp. 2087–2090, 1989.

[FRA 08] FRANCOIS B., LALOUI L., "ACMEG-TS: a constitutive model for unsaturated soils under non-isothermal conditions", *International Journal of Numerical and Analytical Methods in Geomechanics*, vol. 32, pp. 1955–1988, 2008.

[HON 13] HONG P.Y., PEREIRA J.M., TANG A.M., *et al.*, "On some advanced thermo-mechanical models for saturated clays", *International Journal for Numerical and Analytical Methods in Geomechanics*, 2013. DOI: 10.1002/nag.2170.

[HUE 90] HUECKEL T., BALDI G., "Thermo plasticity of saturated clays: experimental constitutive study", *Journal of Geotechnical Engineering*, vol. 116, pp. 1778–1796, 1990.

[HUE 92] HUECKEL T., "On effective stress concepts and deformation in clays subjected to environmental loads: discussion", *Canadian Geotechnical Journal*, vol. 29, pp. 1120–1125, 1992.

[HUE 98] HUECKEL T., PELLEGRINI R., DEL OLMO C., "A constitutive study of thermo-elasto-plasticity of deep carbonatic clays", *International Journal of Numerical and Analytical Methods in Geomechanics*, vol. 22, pp. 549–574, 1998.

[HUE 09] HUECKEL T., FRANCOIS B., LALOUI L., "Explaining thermal failure in saturated clays", *Géotechnique*, vol. 59, no. 3, pp. 197–212, 2009.

[HUJ 79] HUJEUX J.C., Calcul numérique de problèmes de consolidation élastoplastique, Doctoral Thesis, Ecole Centrale, Paris, 1979.

[LAL 93] LALOUI L., Modélisation du comportement thermo-hydro-mécanique des milieux poreux anélastique, Doctoral Thesis, Ecole Centrale de Paris, 1993.

[LAL 03] LALOUI L., CEKEREVAC C., "Thermo-plasticity of clays: an isotropic yield mechanism", *Computers and Geotechnics*, vol. 30, no. 8, pp. 649–660, 2003.

[LAL 08] LALOUI L., CEKEREVAC C., "Non-isothermal plasticity model for cyclic behaviour of soils", *International Journal for Numerical and Analytical Methods in Geomechanics*, vol. 32, no. 5, pp. 437–460, 2008.

[LAL 09] LALOUI L., FRANÇOIS B., "ACMEG-T: soil thermoplasticity model", *Journal of Engineering Mechanics*, vol. 135, no. 9, pp. 932–944, 2009.

[LAN 99] LANCELLOTTA R., CALAVERA J., *Fondazioni*, McGraw-Hill, 1999.

[MCK 65] MCKINSTRY H.A., "Thermal expansion of clay materials", *American Mineralogist*, vol. 50, pp. 210–222, 1965.

[MIL 92] MILIZIANO S., Influenza della temperatura sul comportamento meccanico delle terre coesive, Doctoral Thesis, University of Rome "La Sapienza", Italy, 1992.

[MOD 97] MODARESSI H., LALOUI L., "A thermo-viscoplastic constitutive model for clays", *International Journal for Numerical and Analytical Methods in Geomechanics*, vol. 21, no. 5, pp. 313–315, 1997.

[MOR 95] MORITZ L., Geotechnical properties of clay at elevated temperatures, Report: 47, Swedish Geotechnical Institute, Linköping, 1995.

[NOV 79] NOVA R., WOOD D.M., "Constitutive model for sand in triaxial compression", *International Journal for Numerical and Analytical Methods in Geomechanics*, vol. 3, no. 3, pp. 255–278, 1979.

[PLU 69] PLUM R.L., ESRIG M.I., Some temperature effects on soil compressibility and pore water pressure. Effect of temperature and heat on engineering behaviour of soils, Highway research board special report, vol. 103, pp. 231–242, 1969.

[POT 99] POTTS D.M., ZDRAVKOVIĆ L., *Finite Element Analysis in Geotechnical Engineering: Theory*, Thomas Telford Limited, 1999.

[TID 89] TIDFORS M., SÄLLFORS S., "Temperature effect on preconsolidation pressure", *Geotechnical Testing Journal*, vol. 12, no. 1, pp. 93–97, 1989.

[TOW 93] TOWHATA I., KUNTIWATTANAUL P., SEKO I., *et al.*, "Volume change of clays induced by heating as observed in consolidation tests", *Soil and Foundations*, vol. 33, pp. 170–183, 1993.

[VAN 80] VAN EEKELEN H.A.M., "Isotropic yield surfaces in three dimensions for use in soil mechanics", *International Journal for Numerical and Analytical Methods in Geomechanics*, vol. 4, no. 1, pp. 89–101, 1980.